16.512, Rocket Propulsion
Prof. Manuel Martinez-Sanchez
Lecture 30: Dynamics of Turbopump Systems: The Shuttle Engine

Dynamics of the Space Shuttle Main Engine Oxidizer Pressurization Subsystems

Selected Sub-Model

In the complete SSME engine, all variables affect each other in complex ways. In order to test our fault detection algorithms, a dynamic subsystem is desired, with reduced order, but with the unmodelled states interacting as weakly as possible with those modelled. Attention was focused on the liquid oxygen subsystem for two main reasons:

(a) The O/F ratio at rated power is 6, so that the LOX dynamics should dominate over the LH effects wherever they interact, and

(b) The turbopump pre-burners are run very fuel-rich in order to limit the turbine inlet temperatures below the metallurgical limits of the uncooled blades; small excursions of the LOX flow to the pre-burners are then immediately translated into large and potentially critical turbine temperature excursions.

In our submodel we therefore focus attention on the LOX turbopump, which feeds both, the main LOX injectors, and (after the boost stage) the two turbine pre-burners. Also modeled are the dynamics of the LOX feeding line to the pre-burners, as well as to the main LOX valve and main injector, plus the LOX pre-burner itself and the main chamber pressure. Variations of the LH-related states should indeed couple weakly to the LOX system, mainly through LH flow variations onto the pre-burners (insensitive, since they are fuel-rich), and into the main chamber (choked flow, no feedback).

The Dynamic Equations

There are three types of dynamic equations to be considered:

(1) Rotational dynamics of the LOX turbopumps.

(2) Equations expressing the liquid inertia under pressure difference variations (analogous to inductance in electric circuits).

(3) Equations expressing the ability of cavities to store fluid due to its compressibility under pressure fluctuations (analogous to capacitive effects).

(1) Rotational Dynamics

If I_{OTP} is the moment of the inertia of the Oxidizer Turbo Pump (OTP) rotor, Ω_{02} its angular velocity, τ_{OT_2} the torque delivered by the OTP turbine, τ_{OP_2} the torque absorbed by the main oxidizer pump stage, and τ_{OP_3} the torque absorbed by the oxidizer booster pump, then

$$I_{OTP}\frac{d\Omega_{02}}{dt} = \tau_{OT_2} - \tau_{OP_2} - \tau_{OP_3} \qquad (1)$$

In a hybrid system where Ω_{02} is in rad/sec, t in seconds, and the torque in lb-in, the constant I_{OTP} has a value $\frac{1}{0.916}$ (which implies I_{OTP} = 422 $lb_m in^2$).

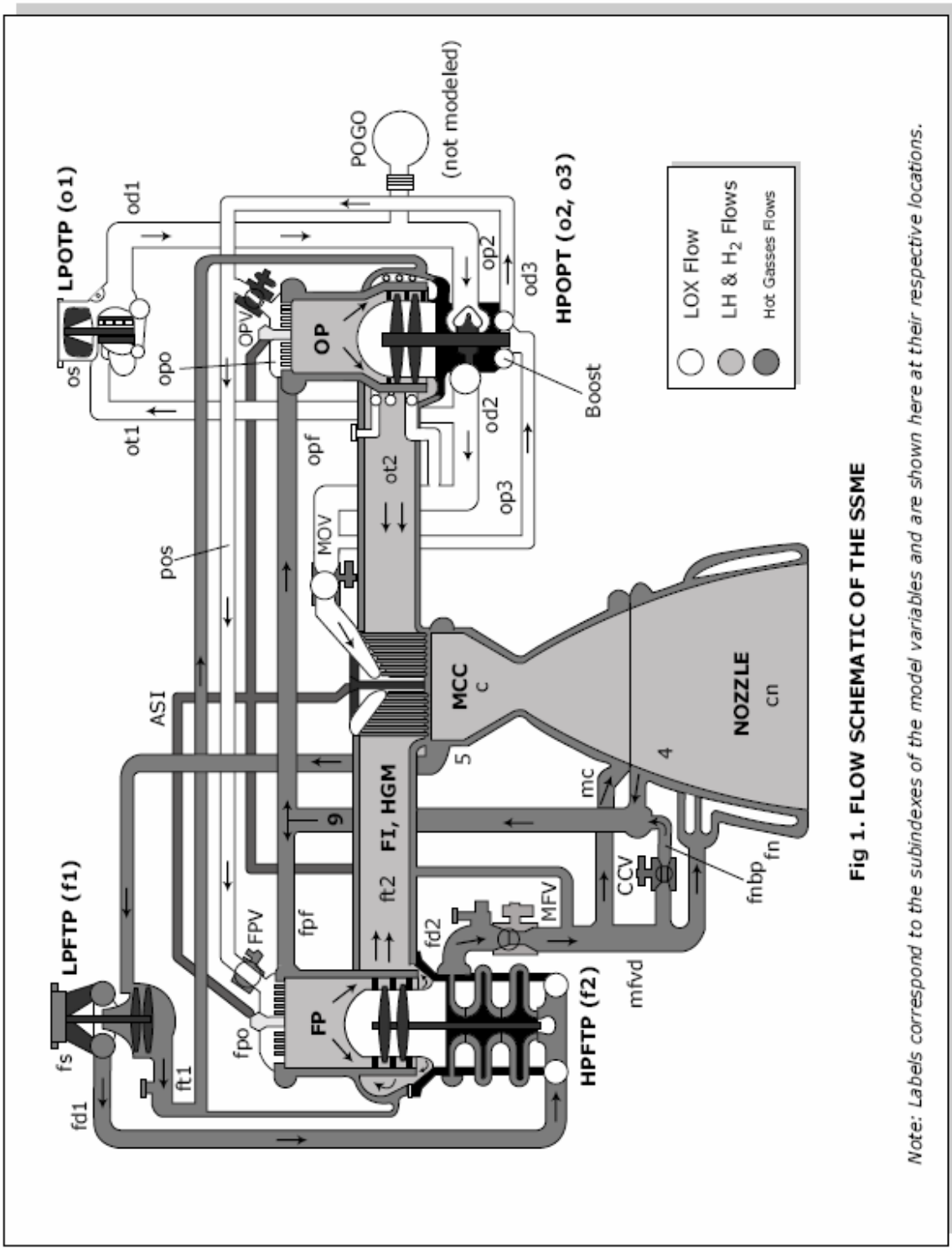

Fig 1. FLOW SCHEMATIC OF THE SSME

Note: Labels correspond to the subindexes of the model variables and are shown here at their respective locations.

(2) Inertia of LOX in pre-burner common supply line

This is a prototypical equation of type (2), and, in order to illustrate the underlying physics, we well give here a brief derivation of it.

Consider a pipe of length L and cross-section A, fed by the booster pump discharge at a pressure P_{OD3}, and having a mean pressure P_{POS} (Pre-burner Oxidizer Supply). Frictional forces along the pipe, and at bends and restrictions, contribute a total pressure drop $\lambda\left(\frac{1}{2}\rho\upsilon^2\right)$, where ρ and υ are the LOX density and velocity, and λ (of order unity) is a pressure loss coefficient. The liquid is then acted on in the forward direction by a net force $\left(P_{OD3} - \lambda\ \frac{1}{2}\ \rho\upsilon^2 - P_{POS}\right)A.$. The mass of liquid in the pipe is ρAL, and we must have

$$\left(\rho AL\right)\frac{d\upsilon}{dt} = \left(P_{OD3} - P_{POS} - \frac{\lambda}{2}\rho\upsilon^2\right)A$$

Now, the flow rate in the pipe is $\dot{m}_{OP3} = \rho\upsilon A$, so the equation can be re-written as

$$L\frac{d\,\dot{m}_{OP3}}{dt} = \left(P_{OP3} - P_{POS} - \frac{\lambda}{2\rho A^2}\ \dot{m}_{OP3}^{\ 2}\right)A$$

or

$$\boxed{\left(\frac{L}{A}\right)\frac{d\,\dot{m}_{OP3}}{dt} = P_{OP3} - P_{POS} - K\,\dot{m}_{OP3}^{\ 2}} \qquad (2)$$

where

$$K = \frac{\lambda}{2\rho A^2} \qquad (3)$$

In units of lb_m / sec for $\dot{m}$ and lb/in^2 for P, the constants have the values $\frac{L}{A} = \frac{1}{100}$, K = 0.000813. This implies $\frac{L}{A} = 3.86\ in^{-1}$ and $\lambda = 0.0261\left[A\left(in\right)\right]^2$.

(3)Fluid Capacitance in preburner LOX supply line

This is a prototypical equation of type (3), and we also provide a derivation below:

Considering again the POS supply line, it receives LOX flow at a rate $\dot{m}_{OP3}$ from the booster pump, and discharges $\dot{m}_{FPO}$ into the fuel preburner (FP) and $\dot{m}_{OPO}$ into the oxidizer pre-burner (OP), plus a small amount $\dot{m}_{OP2C}$ which is diverted to cool the pump. Under dynamic conditions, there is a (generally non-zero) net inflow

$\dot{m}_{OP3} - \dot{m}_{FPO} - \dot{m}_{OPO} - \dot{m}_{OP2C} \equiv \sum \dot{m}$. Let ρV be the mass stored in the pipe, where $V = \frac{\pi D^2}{4} L$ is the volume available. Then we must have

$$\frac{d(\rho V)}{dt} = \sum \dot{m} \tag{4}$$

Even though LOX is a liquid, it has finite compressibility at the very high pressures involved here. This is measured by the thermodynamic parameter

$$K = \frac{1}{\rho}\frac{d\rho}{dP} \approx 5 \times 10^{-10}\ Pa^{-1} \approx 3.4 \times 10^{-6}\, in^2 / lb$$

In general, the volume V also varies slightly under pressure fluctuations, but it can be shown that this effect is secondary. We therefore rewrite (4) as

$$\boxed{\left[(\rho V)_{POS}\left(\frac{1}{\rho}\frac{d\rho}{dP}\right)_{LOX}\right]\frac{dP_{POS}}{dt} = \dot{m}_{OP3} - \dot{m}_{FPO} - \dot{m}_{OPO} - \dot{m}_{OP2C}} \tag{5}$$

In the same units as before, the factor $\left[(\rho V)_{POS}\left(\frac{1}{\rho}\frac{d\rho}{dP}\right)_{LOX}\right]$ has a value of $\frac{1}{38,120}$. Using $\frac{1}{\rho}\frac{d\rho}{dp} \cong 3.4 \times 10^{-6}\, in^2 / lb$, this implies a line volume V = 409 in^3, which combined with previously estimated $L / A = 3.86\ in^{-1}$, yields $L \cong 40\ in$, $A \cong 10\ in^2$. These are not expected to be exact dimensions of the POS line, because the model lumps together several secondary inertios and capacitances, but they do appear reasonable. Incidentally, from the previous result $\lambda \cong 0.0261 A^2_{(in)}$, we now estimate $\lambda \cong 2.8$, again a reasonable value for a pressure loss factor.

The Complete Submodel

In addition to the three equations derived above, there are three others of the fluid inertia type and three others of the fluid capacitance type. The complete submodel, in the same unit used so far, is shown in Table….on next page.

Equations (6), (7), (8) are the ones just derived. Eq. (9) deals with the inertia of the LOX moving through the valve and the injectors of the Fuel Preburner (FP) under the fluctuating drive of the pressure difference $P_{POS} - P_{FP}$, less the pressure drops in the valve and in the injectors. These drops have the characteristic $\dot{m}^2$ form, just as in Eq. (2), but, in addition the valve open area fraction $A / \bar{A}_{FPV}$ appear squared in the denominator, as it should according to Eq. (3). This area fraction will act as one of our control variables.

Eq. (10) is identical in structure to Eq. (9), but refers to the fluid inertia in the LOX dome of the Oxidizer Preburner (OP). Once again, the OP valve area fraction $A / \bar{A}_{OPV}$ appears here as a control variable.

The remaining inertia-type equation is Eq. (13), which refers to the LOX moving through the Main Oxidizer Valve (MOV) under the drive of the difference between the main oxidizer discharge pressure, P_{OD2}, and the main combustor pressure, P_c, less the sum of the pressure drops in the MOV (assumed 100% open) and the injectors.

The remaining three capacitance-type equations are Eqs. (11), (12) and (14). Eq. (11) describes accumulation of gas in the Oxidizer Preburner (OP), with mass flow $\dot{m}_{OPF}$ (the un-modelled fuel flow into the OP) plus $\dot{m}_{OPO}$ (the LOX flow into the OP) entering, and almost all of the gas flow input to the oxidizer turbine, $\dot{m}_{OT2}$, leaving.

Table: DYNAMICS OF LOX PRESSURIZATION SUBSYSTEM

Equation No.	Equation	Description	Time Constant (sec.)
(6)	$\frac{1}{0.916}\frac{d\Omega_{O2}}{dt} = \tau_{OT2} - \tau_{OP2} - \tau_{OP3}$	Rotational dynamics of OTP	0.058
(7)	$\frac{1}{100}\frac{^{din}OP3}{dt} = P_{OD3} - P_{POS} - 0.000813\,\dot{m}^{2}_{OP3}$	LOX inertia in preburner supply line	0.00013
(8)	$\frac{1}{38120}\frac{^{dP}POS}{dt} = \dot{m}_{OP3} - \dot{m}_{FPO} - \dot{m}_{OPO} - \dot{m}_{OP2C}$	Mass storage in preburner supply line	0.0020
(9)	$\frac{1}{2}\frac{^{d\dot{m}}FPO}{dt} = P_{POS} - P_{FP} - 0.02488\left(\frac{\dot{m}_{FPO}}{A / A_{FPV}}\right)^2 - 0.1948\,\dot{m}^{2}_{OPO}$	LOX inertia in injector dome of FP	0.0048
(10)	$\frac{^{din}OPO}{dt} = P_{POS} - P_{OP} - 0.260\left(\frac{\dot{m}_{OPO}}{A / A_{OPV}}\right)^2 - 1.463\,\dot{m}^{2}_{OPO}$	LOX inertia in injector dome of OP	0.0034
(11)	$\frac{1}{10,000}\frac{^{dP}OP}{dt} = \dot{m}_{OPF} + \dot{m}_{OPO} - 0.9980\,\dot{m}_{OT2}$	Mass storage in Oxidizer Preburner	0.0143
(12)	$\frac{1}{3000}\frac{^{dP}F1}{dt} = \dot{m}_{FT1} + \dot{m}_{OT2} + M_{FT2} - 1.085\,\dot{m}_{OT2}$	Mass storage in fuel ducts to injector	0.0050
(13)	$\frac{1}{25}\frac{^{d\dot{m}}MOV}{dt} = P_{OD2} - P_C - 0.001715\,\dot{m}^{2}_{MOV}$	LOX inertia in main injector dome	0.0078
(14)	$\frac{1}{4000}\frac{dP_c}{dt} = \dot{m}_{F1} + \dot{m}_{MOV} - \dot{m}_{CN}$	Mass storage in main combustor	0.00074

Equation (12) describes the gas accumulation in the two large ducts which bring the partially oxidized hydrogen to the main chamber injector dome. Feeding this volume are the (unmodelled) discharge flows on the main Fuel Turbine $\left(\dot{m}_{FT2}\right)$ and of the low pressure Fuel Turbine $\dot{m}_{FT1}$, plus the discharge of the main Oxidizer Turbine, $\left(\dot{m}_{OT2}\right)$; leaving this volume is basically the main Fuel Injector flow $\left(\dot{m}_{FI}\right)$, plus some smaller LH cooling flows, up to 1.085 $\dot{m}_{FI}$.

Finally, Eq. (14) governs the changes in the main combustor pressure, P_c, due to mass accumulation. The mass inputs are the fuel and oxidizer injector flows ($\dot{m}_{FI}, \dot{m}_{MOV}$), while the mass loss is the nozzle flow rate $\dot{m}_{CN}$.

Characteristic Times

For each of the dynamic equations (6)-(14), we can estimate the characteristic time constant, which provides same preliminary appreciation for the dynamics of the system. For this purpose, we balance the rate term with one of the dominant terms on the right; for instance, for Eq. (6), the time constant is $\tau = \frac{\Omega_{O2}}{0.912\tau_{OT2}}$, with Ω_{O2} and τ_{OT2} evaluated at their nominal values (rated power). These time constraints are included in Table…. The preburner supply line flow and the main combustor pressure are seen to adjust rapidly (under 1 msec). Filling and emptying of the Oxidizer Preburner is relatively slow (14 msec), and the shaft speed of the OTP is very slow (58 msec). All other dynamics are comparable in speed with time constants of a few msec.

Calculation of non-state variables

The sequence of algebraic computations (no additional dynamics) required to calculate the right-hand-sides of Eqs. (6)-(14) is summarized in Appendix…. The data for these calculations are the values of the nine state variables, the values of the control variables (preburner valve openings), and a few unmodelled variables arising from the fuel side of the overall system. The latter are generally kept at their nominal values.

Appendix B. Steady State Values from the SSME Thermodynamic Model

Variable	State	Description	Units	65% RPL	100% RPL	104% RPL	109% RPL
x_fpv	Cntrl	Fuel preburner valve	fraction	0.692	0.782	0.802	0.820
x_opv	Cntrl	Oxidizer preburner valve	fraction	0.543	0.641	0.659	0.683
x_mov	Cntrl	Main oxidizer valve	fraction	1.000	1.000	1.000	1.000
x_mfv	Cntrl	Main fuel valve	fraction	1.000	1.000	1.000	1.000
x_ccv	Cntrl	Coolant control valve	fraction	0.664	1.000	1.000	1.000
omega_f1	x	LPFTP turbine speed	rad/sec	1,491.8	1,634.6	1,671.5	1,722.0
omega_f2	x	HPFTP turbine speed	rad/sec	2,824.3	3,596.6	3,695.6	3,822.2
omega_o1	x	LPOTP turbine speed	rad/sec	419.2	527.5	540.4	556.7
omega_o2	x	HPOTP turbine speed	rad/sec	2,049.3	2, 856.6	2,947.0	3,059.0
t_4		Fuel temp. inside nozzle HE	R	449.5	465.8	456.4	448.1
t_5		Fuel temp. inside MCC HE	R	509.0	466.0	455.9	443.1
t_9		Preburners fuel supply line temp.	R	295.4	276.4	276.4	276.5
t_op		Oxidizer preburner temperature	R	1,057.0	1440.3	1,475.8	1,517.6
t_fp		Fuel preburner temperature	R	1,633.5	1,753.9	1,796.1	1,854.8
t_fi		Fuel injector temperature	R	1,392.7	1,560.7	1,593.1	1,636.2
t_c		Main Chamber (MCC) temperature	R	6,400 . 0	6,400.0	6,400.0	6,400.0
tw_15	x	Hot wall temp. at MCC HE	R	1,228.8	1214.9	1,203.1	1,187.1
tw_25	x	Cold wall temp. at MCC HE	R	509.0	466.0	455.9	443.1
tw_14	x	Hot wall temp. at nozzle HE	R	1,162.5	1,260.3	1,250.4	1,244.5
tw_24	x	Cold wall temp. at nozzle HE	psia	449.5	465.8	456.4	448.1
p_od1		LPOTP discharge pressure	psia	334.5	410.3	418.6	430.4
p_od2		HPOTP discharge pressure	psia	2440.4	4110.3	4,314.3	4,573.0
p_od3		HPOTP boost discharge pressure	psia	4,089.5	6,985.3	7,316.2	7,750.8
p_fd1		LPFTP discharge pressure	psia	256.1	287.1	296.7	310.0
p_fd2		HPFTP discharge pressure	psia	3, 910.1	6.095.5	6,415.1	6,834.8
p_pos	x	OP and FP supply line discharge	psia	4,087.6	6,978.7	7,308.6	7,741.8
p_op	x	Oxidizer preburner pressure	psia	2,884.4	5,047.5	5,326.0	5,685.7
p_fp	x	Fuel preburner pressure	psia	2,956.4	4976.9	5,251.8	5,611.4
p_fi	x	Fuel injector pressure	psia	2,064.1	3,230.0	3,369.1	3,545.3
p_c	x	Main chamber pressure	psia	1,953.9	3,006.0	3,126.2	3,276.5
p_cl	x	Coolant liner pressure	psia	2,094.4	3,277.0	3,419.0	3,599.2
p_4		Nozzle heat exchanger (HE) press.	psia	3,266.1	5,594.1	5,928.0	6,348.7
p_5		MCC heat exchanger pressure	psia	3,008.6	4,675.4	4,904.5	5,202.3
p_9	x	Preburners fuel supply line press.	psia	3,243.4	5,499.6	5,793.6	6,175.1
p_os	x	LPOTP pump inlet pressure	btu/lbm	103.5	99.9	99.5	99.0
su_4	x	Fuel sp. int. energy at nozzle HE	btu/lbm	1,003.5	1,037.3	1,008.5	983.1
su_5	x	Fuel sp. int. energy at MCC HE	Btu/sec	1,171.8	1,042.0	1,012.5	974.7
dg_14		Hot wall to fuel HFR ar nozzle HE	Btu/sec	54,860.5	75,959.2	78,543.1	81,662.9
dg_24		Cold wall to fuel HFR at nozzle HE	Btu/sec	0.362	0.362	-0.362	-0.363
dg_tc4		Hot gas to wall HFR at nozzle HE	Btu/sec	54, 859.8	75,959.2	78,543.8	81,663.5
dg_15		Hot wall to fuel HFR at MCC HE	Btu/sec	28, 419.2	40,205.2	41,587.3	43,323.0
dg_25		Cold wall to fuel HFR at MCC HE	Btu/sec	0.369	0.367	-0.367	-0.370
dg_tc5		Hot gas to hot wall HFR at MCC HE	Btu/sec	28,418.9	40.204.9	41,587.6	43,323.4
rho_4	x	Fuel density at nozzle HE	lbm/in^3	0.000681	0.001024	0.001089	0.001163
rho_5	x	Fuel density at MCC HE	lbm/sec	0.000566	0.000889	0.000941	0.001009
dm_ft1		LPFTP turbine flow rate	lbm/sec	18.3	28.4	30.1	32.4
dm_ft2		HPFTP turbine flow rate	lbm/sec	84.3	146.2	153.7	163.2
dm_ot1	x	LPOTP turbine flow rate	lbm/sec	132.8	176.0	180.6	186.3
dm_ot2		HPOTP turbine flow rate	lbm/sec	36.9	58.3	61.0	64.5
dm_fd2		HPFTP pump fuel flow rate	lbm/sec	93.3	144.5	150.3	157.4
dm_op3	x	HPOTP boost pump LOX flow rate	lbm/sec	52.3	96.7	103.1	111.6
dm_fpo	x	Fuel preburner oxidizer flow rate	lbm/sec	36.1	66.5	71.2	77.4
dm_opo	x	Oxidizer preburner LOX flow rate	lbm/sec	11.2	23.3	24.8	26.7
dm_fpf	x	Fuel preburner fuel flow rate	lbm/sec	47.1	78.3	81.1	84.3
dm_opf	x	Oxidizer preburner fuel flow rate	lbm/sec	25.3	34.9	36.1	37.7
dm_mov	x	Main oxidizer valve flow rate	lbm/sec	532.6	802.4	832.3	869.5
dm_fi	x	Main fuel injector flow rate	lbm/sec	128.6	214.7	225.6	239.7
dm_cli	x	Coolant liner inlet flow rate	lbm/sec	0.526	0.655	0.675	0.702
dm_clo	x	Coolant liner outlet flow rate	lbm/sec	0.526	0.655	0.675	0.702
dm_mc	x	MCC heat exchanger fuel flow rate	lbm/sec	18.3	28.4	30.1	32.4
dm_fn	x	Nozzle HE inlet fuel flow rate	lbm/sec	40.6	52.2	55.1	58.3
dm_4	x	Nozzle HE outlet fuel flow rate	lbm/sec	40.6	52.2	55.1	58.3
m_fnbp	x	Nozzle HE bypass fuel flow rate	lbm/sec	31.8	61.1	62.1	63.7
dm_asifp	x	Fuel preburner ASI flow rate	lbm/sec	0.920	0.969	0.986	1.008
dm_asiop	x	Oxidizer preburner ASI flow rate	lbm/sec	0.977	0.956	0.972	0.996
dm_asimc	x	MCC ASI flow rate	lbm/sec	0.733	0.915	0.944	0.982
dm_os		LPOTP pump inlet flow rate	lbm/sec	584.9	0.944	935.4	981.0
dm_cn		Thrust chamber nozzle flow rate	lbm/sec	662.0	935.4	1,058.9	1,110.1

Appendix C. State Variables in a simulated Throttling Sequence

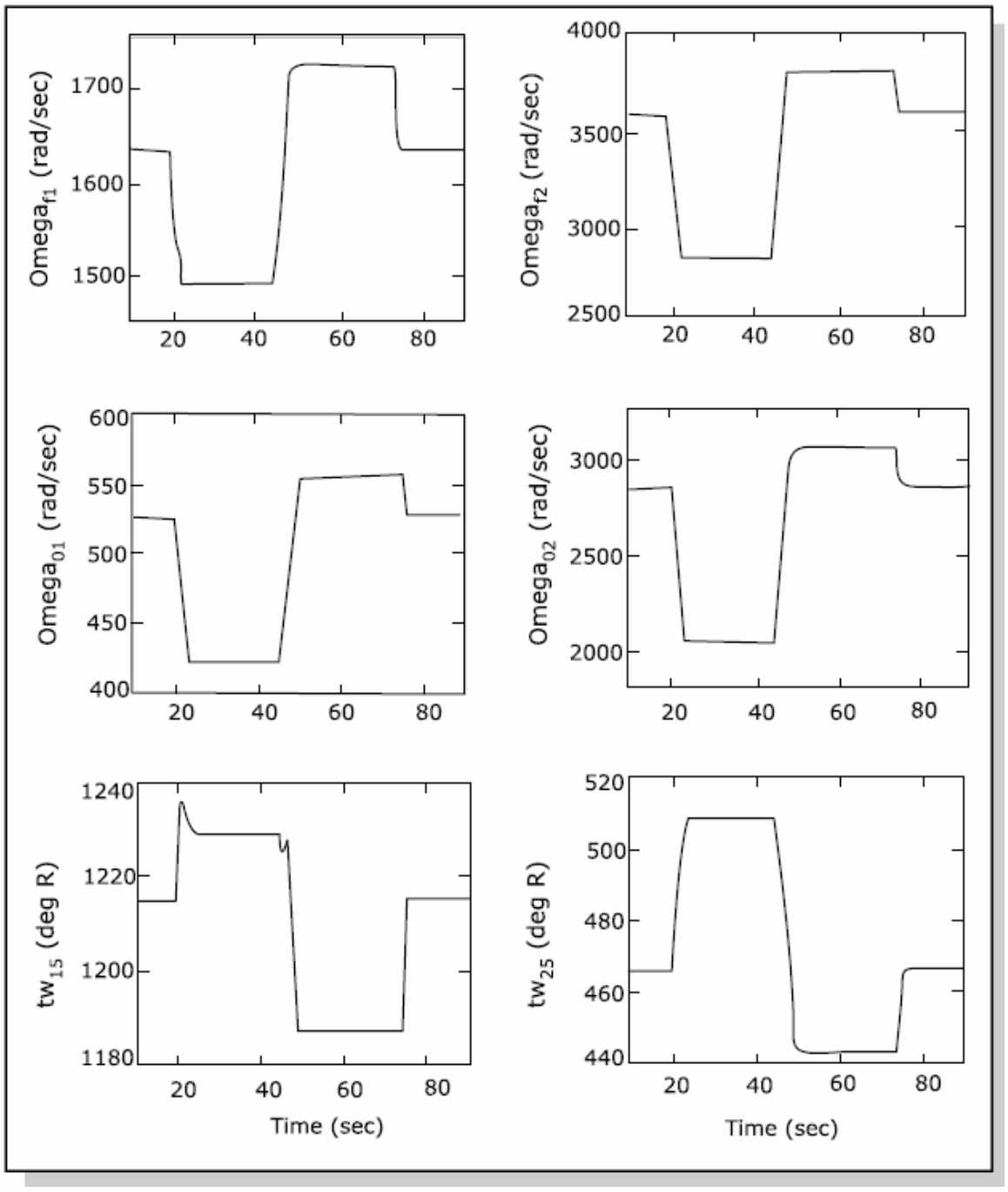

Appendix D. Characteristic Times (approx.) for the SSME Dynamic Model

Variable	*Description*	*Characteristic Time (msec)*	*Dynamic Category*
omega_f1	LPFTP turbine speed	120	very slow
omega_f2	HPFTP turbine speed	105	very slow
omega_o1	LPOTP turbine speed	74.8	very slow
omega_o2	HPOTP turbine speed	57.7	very slow
tw_15	Hot wall temperature at MCC heat exchanger (HE)	98.2	very slow
tw_25	Cold wall temperature at MCC HE	infinite	indeterminate
tw_14	Hot wall temperature at nozzle HE	99.7	very slow
tw_24	Cold wall temperature at nozzle HE	infinite	indeterminate
p_pos	OP and FP LOX supply line pressure	2.0	fast
p_op	Oxidizer preburner pressure	8.5	medium
p_fp	Fuel preburner pressure	2.09	fast
p_fi	Fuel injector pressure	5.0	medium
p_c	Main chamber pressure	0.74	very fast
p_cl	Coolant liner pressure	17.8	slow
p_9	Preburners fuel supply line pressure	4.76	medium
p_os	LPOTP pump inlet pressure	0.75	very fast
su_4	Fuel sp. int. energy at nozzle HE	2.5	fast
su_5	Fuel sp. int. energy at MCC HE	21.1	slow
rho_4	Fuel density at nozzle HE	38.6	slow
rho_5	Fuel density at MCC HE	32.5	slow
dm_ot1	LPOTP turbine flow rate	35.7	slow
dm_op3	HPOTP boost pump LOX flow rate	0.13	very fast
dm_fpo	Fuel preburner oxidizer flow rate	4.82	medium
dm_opo	Oxidizer preburner LOX flow rate	3.36	fast
dm_fpf	Fuel preburner fuel flow rate	0.72	very fast
dm_opf	Oxidizer preburner fuel flow rate	0.64	very fast
dm_mov	Main oxidizer valve flow rate	7.8	medium
dm_fi	Main fuel injector flow rate	20.0	slow
dm_cli	Coolant liner inlet flow rate	1.07	fast
dm_clo	Coolant liner outlet flow rate	1.98	fast
dm_mc	MCC heat exchanger fuel flow rate	0.94	very fast
dm_fn	Nozzle HE inlet fuel flow rate	0.59	very fast
dm_4	Nozzle HE outlet fuel flow rate	0.46	very fast
dm_fnbp	Nozzle HE bypass fuel flow rate	51.5	very slow
dm_asifp	Fuel preburner ASI flow rate	1.63	fast
dm_asiop	Oxidizer preburner ASI flow rate	1.59	fast
dm_asimc	MCC ASI flow rate	1.64	fast
dm_os	LPOTP pump inlet flow rate	376.8	extremely slow

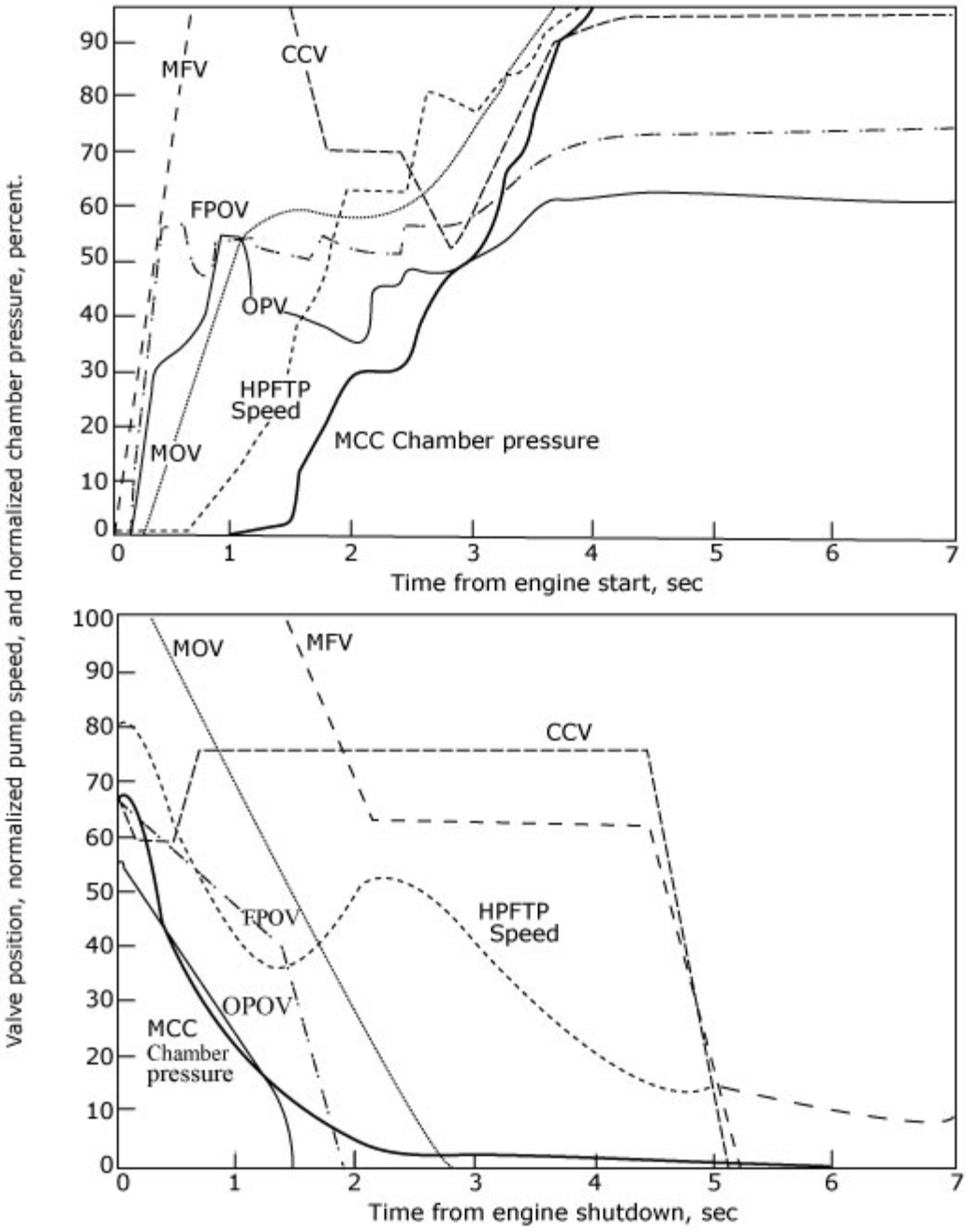

Fig. 10-12. The sequence and events for starting and shutdown of the SSME (Space Shuttle main engine). This particular start sequence leads to a chamber pressure of 2760 psia (normalized here to 100%), a high-pressure fuel turbopump speed of 33,160 rpm (100%), at a sea-level thrust of 380,000 lbf (shown as 100%). This shutdown occurs at altitude when the engine has been throttled to 67% of its power level or a vacuum thrust of 312,559 lbf, which is shown as 67% of the MCC chamber pressure. *(Adapted from The Boeing Company, Rocketdyne Propulsion and Power.)*